Temperature-dependent structural behavior of self-avoiding walks on three-dimensional Sierpinski sponges

Miriam Fritsche* and Dieter W. Heermann
Institute for Theoretical Physics, University of Heidelberg, Philosophenweg 19, 69120 Heidelberg, Germany
(Received 29 March 2010; published 17 May 2010)

The statistics of self-avoiding random walks (SAWs), consisting of up to $N=1280$ steps, on deterministic fractal structures with infinite ramification, modeled by Sierpinski cubic lattices, in the presence of a finite temperature is investigated as a model for polymers absorbed on a disordered medium. Thereby, the three-dimensional Sierpinski sponge is defined by two types of sites with energy 0 and $\epsilon>0$, respectively, yielding a deterministic fractal energy landscape. The probability distribution function of the end-to-end distance of SAWs is obtained and its scaling behavior studied. In the limiting case of temperature $T\to\infty$, the known behavior of SAWs on regular cubic lattices is recovered, while for $T\to 0$ the resulting scaling exponents are confronted with previous calculations for much shorter linear chains based on the exact enumeration technique. For finite temperatures, the structural behavior of SAWs in three dimensions is compared to its two-dimensional counterpart and found to be intermediate between the two limiting cases ($T\to 0$ and $T\to\infty$, respectively), where the characteristic exponents, however, display a nontrivial dependence on temperature.

DOI: 10.1103/PhysRevE.81.051119 PACS number(s): 05.40.−a, 61.41.+e, 61.43.−j

I. INTRODUCTION

Linear polymers made of similar monomer units in a diluted solution display only short-range, repulsive interactions if the solvent is able to screen all long-range forces between them. In such a good solvent, the linear chain can be accurately modeled by a self-avoiding random walk (SAW), for which many statistical properties are known [1,2]. However, much less is known in case of linear polymers embedded in disordered media. In fact, the understanding of how linear polymers behave in a disordered medium, is not only interesting from a theoretical point of view, but it is also relevant for understanding transport properties of polymeric chains in porous media, such as enhanced oil recovery, gel electrophoresis, and gel permeation chromatography [2–4]. Typical examples of models studied so far include SAWs on the incipient percolation cluster [5,6], a random fractal, for which the critical exponents are known only numerically. Despite these achievements, many challenging theoretical issues remain to be understood, among which we draw our attention to the structural behavior of SAWs on deterministic fractals.

However, studying SAWs on substrates displaying self-similarity, one is soon faced with models whose exact solution becomes hard to obtain despite possible approaches such as renormalization group analysis and series expansion. In this work, we focus on Sierpinski carpets [two-dimensional (2D)] and Sierpinski sponges [three-dimensional (3D)], which, being of infinite ramification, are particularly intriguing fractal structures as no renormalization group techniques are known for them. Here, "infinite ramification" refers to the fact that an infinite number of cut operations is necessary to disconnect any given subset of the structure. However, the interest in these fractals extends well beyond possible renormalization group techniques since SAWs on fractal structures have critical exponents which exhibit universality [1]. In this context, it was found that the so-called des Cloizeaux relation [7] neither holds for Sierpinski carpets nor for Sierpinski sponges [8]. In a recent work, one of us has shown that, for two-dimensional Sierpinski lattices, the characteristic exponents display a particular dependence on temperature and consequently on the underlying fractal space [9].

Intrigued by this interesting finding in two dimensions, we study in this work the three-dimensional counterpart. Thus, by investigating SAWs on a Sierpinski sponge in the presence of a finite temperature, we are able to shed some light on the role that the underlying space plays on the statistics of linear polymers. The Sierpinski sponge is defined by allowed sites of energy 0 and by forbidden sites of $\epsilon>0$, therewith yielding a deterministic fractal energy landscape.

SAW configurations are generated via the reptation algorithm [10] modified by a finite acceptance probability $\min\{1,\exp(-\Delta E/T)\}$. Here, ΔE is the energy difference between the attempted and the current configuration. In contrast to the exact enumeration method, the reptation algorithm, even though not exact, allows us to study quite long chain lengths, up to $N=1280$ steps (limited by the size of the fractal lattice that can be generated). It should be noted that there exist other, more involved, accurate algorithms for studying very long SAW chains, as for instance the method by Berretti and Sokal [11] or the pruned-enriched Rosenbluth method by Grassberger [12]. Taking into account the problem of ergodicity known for regular lattices, where certain chain conformations are impossible to occur with a reptation scheme [13], we assess the validity of our results by applying the reptation method to the case of regular lattices in both two and three dimensions, for which the corresponding scaling exponents are well known. From this test, we can conclude that reptation yields accurate results, indicating that possible nonergodic configurations are not important for the present problem, i.e., that the true asymptotic behavior of SAWs can be detected with sufficient accuracy for our present purposes.

The paper is organized as follows: in Sec. II, we summarize the quantities of interest, their scaling functions as well

*fritsche@tphys.uni-heidelberg.de

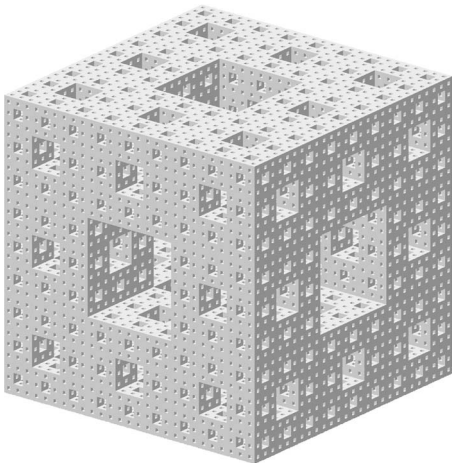

FIG. 1. Illustration of a three-dimensional Sierpinski sponge as obtained after the third iteration. Sites with energy 0 build up the lattice, while those with $\epsilon>0$ represent the lattice's holes.

as the rules of the reptation algorithm. The results are discussed in Sec. III and the conclusions are drawn in Sec. IV.

II. MODEL

SAW configurations of chain lengths up to $N=1280$ steps at various temperatures T are generated on a three-dimensional lattice of linear size $L=3\times 3^6=2187$, corresponding to a Sierpinski sponge of the sixth generation. For our purposes, we chose the most common and symmetric (small lacunarity) Sierpinski cubic lattice, where the central subunit and its six nearest-neighbor subunits are not present [14]. An illustrative example is shown in Fig. 1. In order to generate the energy landscape, the allowed sites are assigned an energy 0, while the forbidden ones are assigned an energy $\epsilon>0$. We minimize boundary effects by applying periodic boundary conditions. The initial SAW configuration is taken as a straight rod along the center hole of the fractal. Before taking data on the spatial SAW conformations the SAW is thermalized by a sufficient number of preliminary reptation steps. Subsequently, all resulting SAW configurations are taken into account when performing the statistical average of the end-to-end distance, including those for which no move of the chain has taken place [10]. The number of reptation steps performed is of the order of 10^{10}–10^{11}.

We apply the reptation algorithm to generate SAW configurations, which consists of two steps: (a) picking up at random one of the two ends of the chain, and (b) choosing one of its nearest-neighbor lattice sites at random as its possible new location. If the nearest-neighbor site is empty, the energy difference ΔE between the attempted and current chain configurations is calculated and the reptation step is performed with probability $\min\{1,\exp(-\Delta E/T)\}$, meaning that the whole chain is moved along its track. Otherwise, or if the nearest-neighbor site is occupied, the chain remains at its actual position (in the special case where the occupied nearest-neighbor site corresponds to the other end of the chain, the site is considered empty since it becomes free once the chain moves as a whole). In any case, the process is repeated from step (a) all over again.

To characterize the spatial extension of SAWs on the square lattice, we consider the topological end-to-end distance ℓ after N steps of the walk. The distance ℓ between two points located at coordinates $\{x_1,y_1,z_1\}$ and $\{x_2,y_2,z_2\}$ is defined as

$$\ell = |x_1 - x_2| + |y_1 - y_2| + |z_1 - z_2|. \tag{1}$$

The present ℓ metric is equivalent to the more standard Euclidean or r metric, i.e., $r=\sqrt{(x_1-x_2)^2+(y_1-y_2)^2+(z_1-z_2)^2}$. From a computational point of view it has the advantage that fluctuations are smaller, therewith permitting a more accurate determination of the characteristic exponents defined below.

The end-to-end distance $\ell(N,T)$ for a given temperature T, averaged over all SAW configurations of N steps, denoted as $\bar{\ell}(N,T)$, obeys the scaling relation [15]

$$\bar{\ell}(N,T) \sim N^{\nu(T)} \quad N \gg 1, \tag{2}$$

which defines the possibly temperature-dependent Flory exponent $\nu(T)$. The probability distribution function for the end-to-end distance for a given temperature T, $P(\ell|N,T)$, normalized according to $\int P(\ell|N,T)\mathrm{d}\ell=1$, also obeys a scaling form given by

$$P(\ell|N,T) = \frac{\Omega B(T)}{\ell} F\left(\frac{\ell}{\bar{\ell}(N,T)},T\right), \tag{3}$$

where the factor $\Omega=4\pi$ comes from the angular integration and $F(x,T)$ is the temperature-dependent scaling function

$$F(x,T) = \begin{cases} x^{g_1(T)+\tilde{d}(T)} & \text{for } x \ll 1 \\ x^{g_2(T)+\tilde{d}(T)} \exp[-b(T)x^{\delta(T)}] & \text{for } x \gg 1, \end{cases} \tag{4}$$

defining the possibly temperature-dependent characteristic exponents $g_1(T)$, $g_2(T)$, and $\delta(T)$. The effective temperature-dependent fractal dimension $\tilde{d}(T)$ of the substrate, which enters Eq. (4), is given by

$$\tilde{d}(T) = \frac{\ln[20+\exp(-\epsilon/T)]}{\ln 7}. \tag{5}$$

It takes into account that, for finite temperature T, the sites with energy $\epsilon>0$ are accessed with a finite probability $\exp(-\epsilon/T)$, so that, on average, the accessible area $A(\ell,T)$ within some distance ℓ increases as $A(\ell,T)\propto \ell^{\tilde{d}(T)}$. Note that, for $T\to 0$ and $T\to\infty$, the correct fractal dimensions $\tilde{d}(T=0)=\ln 20/\ln 7$ (Sierpinski sponge) and $\tilde{d}(T=\infty)=\ln 21/\ln 7=3$ (regular square lattice) are obtained.

III. RESULTS

We first analyze the average end-to-end distance $\bar{\ell}(N,T)$ of the SAWs for various chain lengths N and temperatures T according to Eq. (2) in order to determine the Flory exponent $\nu(T)$ as a function of temperature T. In Fig. 2, we show $\nu(T)$ vs temperature T, where $\nu(T)=0.59$ is found independent of T. This is consistent with the expected values $\nu(T\to 0)\cong 0.588$ and $\nu(T\to\infty)\cong 0.58\pm 0.03$ [14]. Thus, we assume a constant value of $\nu(T)$ in the following.

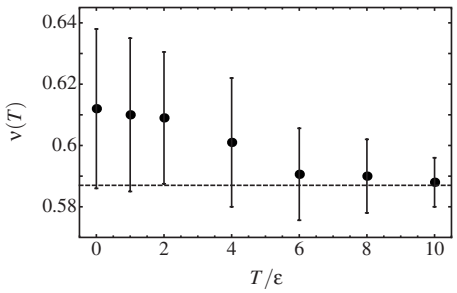

FIG. 2. Plot of the Flory exponent $\nu(T)$ vs temperature T. The behavior is consistent with a temperature-independent value of $\nu(T) \cong 0.588$, shown as the horizontal line. The estimated values are based on simulations for $N=160$, 320, 640, and 1280 with the error bars indicating the estimated error

We discuss the analysis of the distribution function $P(N,T)$ with the goal of determining the characteristic exponents $g_1(T)$, $g_2(T)$ as well as $\delta(T)$ as a function of temperature T. In Fig. 3, we exemplify this analysis by showing the distribution function for the longest chain length studied, $N=1280$, and three temperatures $T=\infty$ (corresponding to the regular cubic lattice), $T=\epsilon$ and $T=0$ (corresponding to the Sierpinski sponge). The value of the characteristic exponent $g_1(T)$ is determined from such plots for various chain lengths

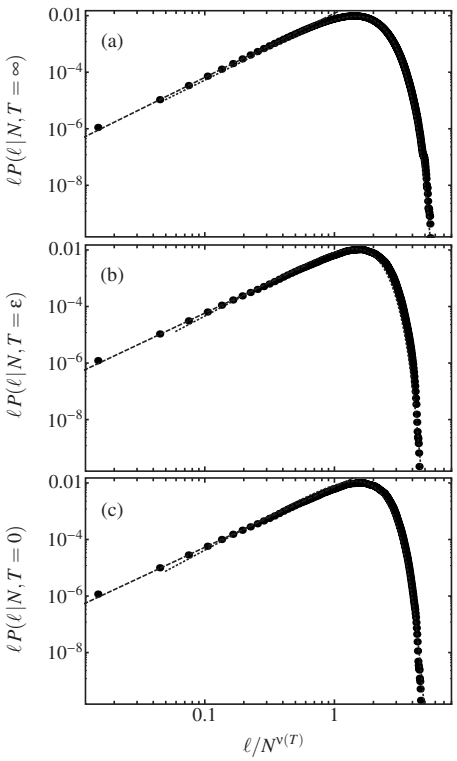

FIG. 3. Plot of the distribution function $\ell P(\ell|N,T)$ vs $\ell/N^{\nu(T)}$, exemplified for $N=1280$ and three values of temperature T: (a) $T=\infty$ (regular square three-dimensional lattice), (b) $T=\epsilon$, and (c) $T=0$ (Sierpinski sponge). The functional form obtained for $\ell/N^{\nu(T)} \ll 1$ is determined by the characteristic exponent $g_1(T)$ and shown as the dashed line, whereas the functional form for $\ell/N^{\nu(T)} \gg 1$ is determined by the exponents $g_2(T)$ and $\delta(T)$ and displayed as the dotted line.

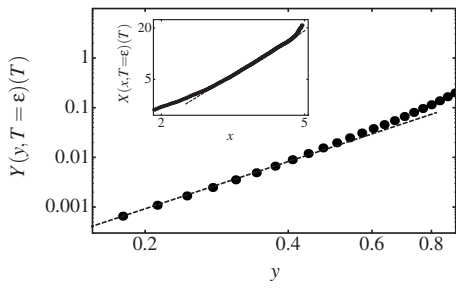

FIG. 4. Plot of the scaling function $Y(y,T)$ vs y, which is expected to scale as $Y(y,T) \propto y^{g_2(T)+\tilde{d}(T)}$ for a properly chosen value of $\delta(T)$. The fit is shown as the dashed line. The inset shows a detailed plot to estimate the accuracy of the obtained value of $g_2(T)$, where $X(x,T)$ is expected to scale as $X(x,T) \propto x^{\delta(T)}$.

N and temperatures T by fitting the slope of the part $\ell/N^{\nu(T)} \ll 1$.

The characteristic exponents $g_2(T)$ and $\delta(T)$, governing the behavior of the distribution function for $\ell/N^{\nu(T)} \gg 1$, need to be determined in a more careful way by separating the power law from the exponential regime in the distribution function. Here, we exploit the normalization $\int P(\ell|N,T)\mathrm{d}\ell = 1$ and the fact that the second moment $\int \ell^2 P(\ell|N,T)\mathrm{d}\ell = N^{2\nu(T)}$ to determine the constants $b(T)$ and $B(T)$ in Eqs. (3) and (4). Then, by plotting the distribution function as

$$Y(y,T) \equiv [b(T)]^{[g_2(T)+\tilde{d}(T)]/\delta(T)}(\Omega B)^{-1}\ell P(\ell|N) \times \exp[-([b(T)]^{1/\delta(T)}\ell/N^{\nu(T)})^{\delta(T)}]$$

versus $y \equiv [b(T)]^{1/\delta(T)}\ell/N^{\nu(T)}$ in a double logarithmic plot, the exponent $g_2(T)$ can be read off from the relation $Y(y,T) \propto y^{g_2(T)+\tilde{d}(T)}$ and adjusted until the above relations Eqs. (3) and (4) are satisfied. The accuracy of the results obtained this way can be assessed by plotting

$$X(x,T) \equiv -\ln\{[b(T)]^{[g_2(T)+\tilde{d}(T)]/\delta(T)}[\Omega B(T)]^{-1}\ell P(\ell|N,T) \times ([b(T)]^{1/\delta(T)}\ell/N^{\nu(T)})^{-[g_2(T)+\tilde{d}(T)]}\}$$

versus $x \equiv [b(T)]^{1/\delta(T)}\ell/N^{\nu(T)}$ in a double logarithmic plot, from which the exponent $\delta(T)$ can be determined, since it is expected to scale as $X(x,T) \propto x^{\delta(T)}$ (for details of this analysis see [6]). As an example, we show in Fig. 4 the scaling ansatz for chain length $N=1280$ and temperature $T=\epsilon$.

Applying the analysis discussed above, we determine the values for $g_1(T)$, $g_2(T)$, as well as $\delta(T)$ for various temperatures T and chain lengths N. The numerical results for $g_1(T)$ and $g_2(T)$ are shown in Fig. 5 and display a nontrivial behavior between the known limiting cases $T \to 0$ (corresponding to the Sierpinski sponge) and $T \to \infty$ (corresponding to the regular cubic lattice), indicated by dashed lines. Regarding the values $g_1(T=0)=0.38\pm0.02$ and $g_2(T=0)=0.42\pm0.036$, they have to be compared with the critical exponents obtained by exact enumeration $g_1^{\mathrm{EE}}(T=0)=0.16\pm0.05$ and $g_2^{\mathrm{EE}}(T=0)=0.1\pm0.05$ [14]. It should be noted that the discrepancy between the respective critical exponents can be attributed to the different chain lengths considered in each calculation, as we studied chain lengths up to

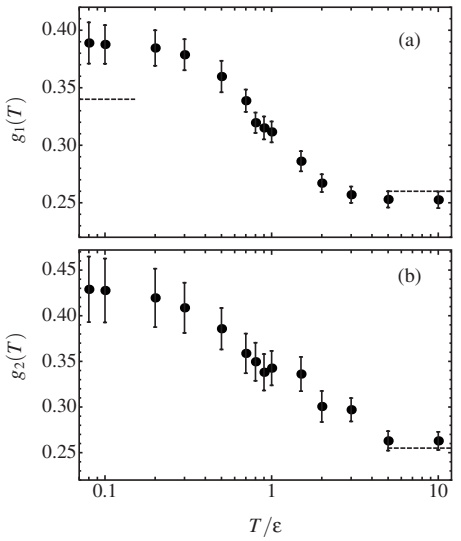

FIG. 5. Plot of the characteristic exponents (a) $g_1(T)$ and (b) $g_2(T)$ vs temperature T. The known limiting cases $T\to 0$ (Sierpinski sponge) and $T\to\infty$ (regular square lattice) are shown as dashed horizontal lines. The estimated values are based on simulations for $N=160$, 320, 640, and 1280, with the error bars indicating the estimated error.

$N=1280$ in contrast to the much shorter exact enumeration chain lengths. The present data are however consistent with a recent work, where the critical exponent $g_1(T=0)=0.33\pm0.05$ has been determined both by the reptation method alone as well as by the mixing of reptation with pivot moves [8]. Corresponding to the previously studied two-dimensional Sierpinski carpet, in three dimensions $g_1(T)$ decreases significantly earlier than $g_2(T)$ as temperature T is increased. This indicates that the probability of compact SAW configurations [which is mainly determined by $g_1(T)$] is much more influenced by a finite temperature T than the probability of SAW configurations of medium size [which is mainly determined by $g_2(T)$].

In Fig. 6, we display the numerically obtained values for $\delta(T)$. Note that the apparent decrease in $\delta(T)$ with T might be explained by the apparent decrease in $\nu(T)$ with T (cf. Fig. 2) according to the Fisher relation. From our simulations, we conclude that $\delta(T)$ is approximately independent of T, which means that the probability of elongated SAW configurations is not (or hardly) influenced by a finite temperature T.

IV. DISCUSSION

We study the statistics of SAWs on deterministic fractal structures with infinite ramification modeled by three-dimensional Sierpinski cubic lattices in the presence of a finite temperature, therewith creating a deterministic fractal energy landscape. By extensive reptation simulations, we measure the average spatial extension of the SAWs in this energy landscape for various chain lengths N and temperatures T, and determine the characteristic exponents $\nu(T)$, $g_1(T)$, $g_2(T)$, and $\delta(T)$ as functions of temperature T. In the limiting case of temperature $T\to\infty$, the known behavior of SAWs on regular cubic lattices is recovered. For $T=0$, the obtained value for $g_1(T=0)=0.38\pm0.02$ is in agreement with a previous work applying both the reptation method alone and a mixing of reptation with pivot moves. To our knowledge this is the first report of $g_2(T=0)=0.42\pm0.036$ for chain lengths up to $N=1280$. For finite temperatures, the structural behavior is found to be intermediate between the two limiting cases: Since $g_1(T)$ decreases significantly earlier as temperature T is increased, the probability of compact SAW configurations [which is mainly determined by $g_1(T)$] is much more influenced by a finite temperature T than the probability of SAW configurations of medium size [which is mainly determined by $g_2(T)$].

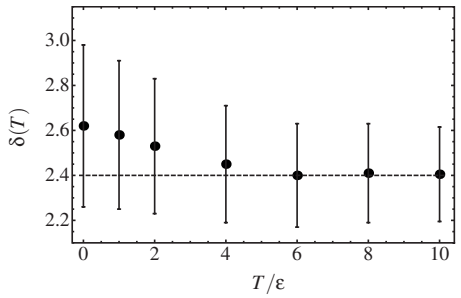

FIG. 6. Plot of the characteristic exponent $\delta(T)$ vs temperature T. The known value $\delta(T=\infty)\cong 2.4$ is shown as the dashed horizontal line. The estimated values are based on simulations for $N=160$, 320, 640, and 1280, with the error bars indicating the estimated error.

ACKNOWLEDGMENTS

M.F. gratefully acknowledges funding from the Heidelberg Graduate School of Mathematical and Computational Methods for the Sciences (HGS MathComp). M.F. thanks Danilo Piparo for fruitful discussions. For this work, the bwGRiD parallel computing facilities (http://www.bw-grid.de), member of the German D-Grid initiative, funded by the Ministry for Education and Research and the Ministry for Science, Research and Arts Baden-Wuerttemberg, as well as the high performance PC cluster HELICS II at the Interdisciplinary Center for Scientific Computing (IWR) were used.

[1] P. G. de Gennes, *Scaling Concepts in Polymer Physics* (Cornell University Press, New York, 1979).
[2] M. Doi and S. F. Edwards, *The Theory of Polymers Dynamics* (Clarendon, Oxford, 1986).
[3] F. A. L. Dullien, *Porous Media, Fluid Transport and Pore Structure* (Academic, New York, 1979).
[4] A. T. Andrews, *Electrophoresis: Clinical Applications* (Oxford University Press, New York, 1986).
[5] D. ben-Avraham and S. Havlin, *Diffusion and Reactions in Fractals and Disordered Systems* (Cambridge University Press, Cambridge, England, 2000).
[6] A. Ordemann, M. Porto, H. E. Roman, S. Havlin, and A.

Bunde, Phys. Rev. E **61**, 6858 (2000).
[7] J. des Cloizeaux, Phys. Rev. A **10**, 1665 (1974).
[8] F. Marini, A. Ordemann, M. Porto, and H. E. Roman, Phys. Rev. E **74**, 051102 (2006).
[9] M. Fritsche, H. E. Roman, and M. Porto, Phys. Rev. E **76**, 061101 (2007).
[10] F. Mandel, J. Chem. Phys. **70**, 3984 (1979).
[11] A. Berretti and A. Sokal, J. Stat. Phys. **40**, 483 (1985).
[12] P. Grassberger, Phys. Rev. E **56**, 3682 (1997).
[13] N. Madras and A. Sokal, J. Stat. Phys. **47**, 573 (1987).
[14] A. Ordemann, M. Porto, and H. E. Roman, J. Phys. A **35**, 8029 (2002).
[15] P. Flory, J. Chem. Phys. **17**, 303 (1949).